



## **Severely Corroded Reinforced Concrete with Cover Spalling: Part 1. Crack Initiation, Crack Propagation and Cover Delamination**

Downloaded from: <https://research.chalmers.se>, 2019-05-26 11:21 UTC

Citation for the original published paper (version of record):

Coronelli, D., Zandi, K., Lundgren, K. et al (2010)

Severely Corroded Reinforced Concrete with Cover Spalling: Part 1. Crack Initiation, Crack Propagation and Cover Delamination

RILEM Bookseries, 5: 195-205

N.B. When citing this work, cite the original published paper.

Coronelli, D., Zandi Hanjari, K., Lundgren, K. and Rossi, E. (2010). Severely corroded reinforced concrete with cover spalling: Part 1. Crack initiation, crack propagation and cover delamination. *Joint Fib-RILEM Workshop on Modelling of Corrosion Concrete Structures*, 22–23 Nov., Madrid, Spain.

# Severely Corroded Reinforced Concrete with Cover Cracking: Part 1. Crack Initiation and Propagation

Dario Coronelli <sup>1</sup>, Kamyab Zandi Hanjari <sup>2</sup>, Karin Lundgren <sup>2</sup>, Enrico Rossi <sup>1</sup>

<sup>1</sup> Politecnico di Milano, Dipartimento di Ingegneria Strutturale, Italy

<sup>2</sup> Chalmers University of Technology, Department of Civil and Environmental Engineering, Sweden

**Abstract.** In many corroding RC structures, it is not uncommon that cover spalling and delamination have occurred. Previous research has been mainly concerned with lower corrosion levels leading to cover cracking. Moreover, the main focus of the available knowledge concerns the corrosion of the main reinforcement; while the corrosion of the stirrups is often overlooked. In an experimental investigation, corrosion attack causing crack initiation, propagation and cover delamination are measured. The specimens have the shape of a beam-end and are corroded with an accelerated method. The location of the bar, middle and corner placement; the amount of transverse reinforcement; the corrosion level of longitudinal reinforcement and of transverse reinforcement are studied. The specimens after corrosion are also used in pull-out bond tests; the results are presented in a companion paper subtitled “Part 2. Anchorage Capacity”. The first test results of the ongoing experimental campaign are presented. The crack patterns are analysed, showing differences between specimens with or without stirrups and when stirrups are corroding or not. Finally, the effect of corrosion was simulated as the expansion of corrosion products in a finite element model and the results, mainly the crack pattern, were compared with the test results. The conclusions address the importance of taking into consideration both high corrosion levels and the corrosion of the stirrups for the assessment of deteriorated structures.

## Introduction

Corrosion of steel reinforcement is one of the most common causes of deterioration of reinforced concrete. Some existing concrete structures like parking garages, harbours and bridges show significant corrosion; it is not uncommon that cover spalling has occurred.

Previous research [1] has been mainly concerned with corrosion levels leading to cover cracking; while relatively little attention has been devoted to higher levels of corrosion causing cover delamination. This is a practically important problem, both for assessment of the residual load-carrying capacity of corrosion-damaged concrete structures, but also for lifetime design of new structures.

Moreover, the main focus of the available knowledge concerns with the corrosion of the main reinforcement; while the corrosion of the stirrups is often overlooked. Field investigations have showed that cover delamination is more probable in areas of tightly spaced stirrups. A rather common approach in modelling the effect of the corroded stirrups is to consider the loss of the cross-sectional area. However, if the effect of corroded stirrups on crack initiation, crack propagation and cover delamination is not considered, this will lead to overestimation of the load-carrying capacity of the corroded structure.

Accelerated corrosion tests are widely used in the laboratory to study the mechanical properties of deteriorated RC specimens. The chemo-physical effects are different from those of natural corrosion [2]. From the mechanical point of view, some concerns exist regarding spurious bond deterioration obtained with high current densities. This study assumes that a sufficiently slow accelerated corrosion test can produce cross-section loss, concrete cracking and bond deterioration approximating natural corrosion, as far as the mechanical effects on RC structures are concerned.

This first of a two part paper presents the accelerated corrosion tests (part 1) on beam-end specimens used for bond tests (part 2). The specimens and the corrosion setup are described. Specimens with or without stirrups were cast; for the former, a part of the specimens had the stirrups protected from the corrosion process, whereas the others had both main steel and stirrup corrosion. Results shown in this paper regard the concrete cracking, crack patterns and reinforcement corrosion.

## Experimental Setup

The specimens have the shape of a beam-end after inclined shear cracking (Fig.1). The concrete specimens were reinforced with the main longitudinal reinforcement of 20 mm diameter and the transverse reinforcement of 8 mm. Since delamination of concrete cover due to corrosion was desired, a relatively small concrete cover, 1.5 times the main bar diameter, was used. The main bars are in contact with the concrete over a 210mm length. The concrete was an ordinary type with average cubic strength 37.5 MPa without chlorides and 34.3 MPa in the mix with 3% chlorides of the specimens with corrosion.

The influences of the location of the anchored bar, middle and corner placement; the presence or not of transverse reinforcement; the corrosion level of longitudinal reinforcement and corrosion of transverse reinforcement were studied.

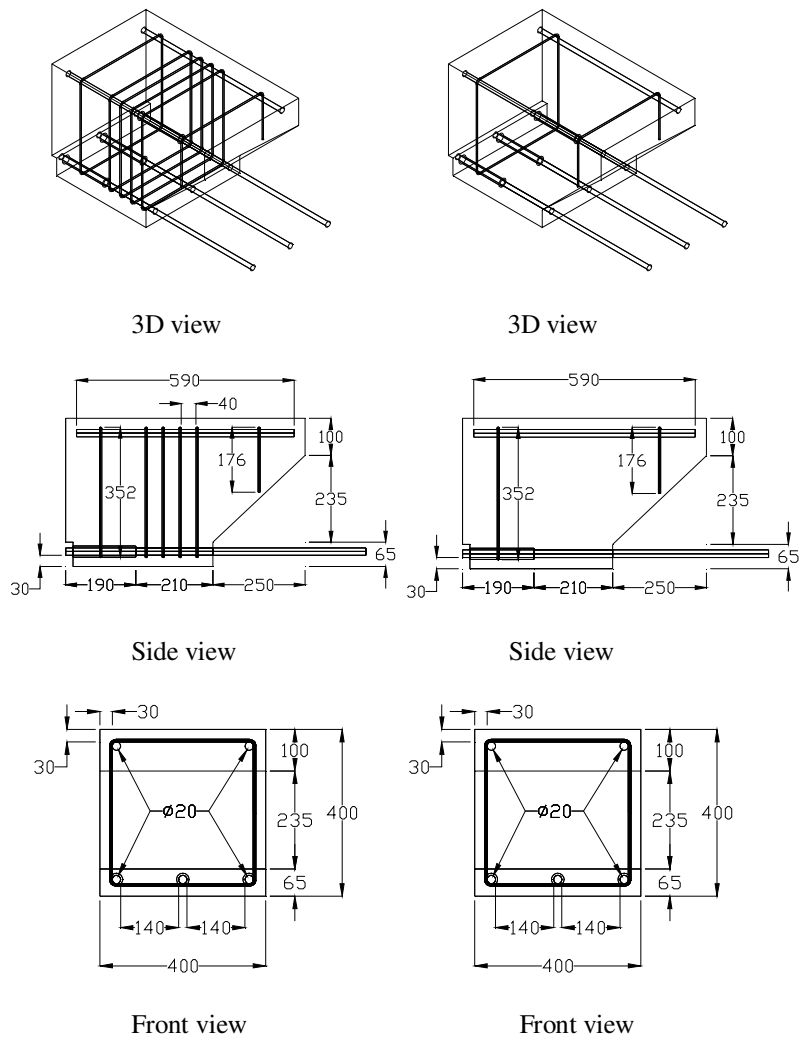


Figure 1. Specimen geometry and reinforcement with transverse reinforcement in the bonded zone of the main reinforcement (left) and without (right).

The specimens were corroded with an electrochemical method, using impressed current (Fig.2). The current flowed through the main bars across the concrete cover to a cathode placed at the bottom of the beam, inside a tank containing a solution

of 3% chlorides. The stirrups in specimens Type A were isolated using electrical tape to avoid corroding. The current density was low (average value  $1,43 \text{ A/m}^2$ ). Test results shown here were corroded for 7 months, obtaining approximately 1% weight loss for each month. Amongst artificial corrosion tests in the literature, this can be considered a low value. Other researches used faster rates, by even one order of magnitude, but spurious mechanical concrete-steel bond deterioration has been measured for high current density values [2].

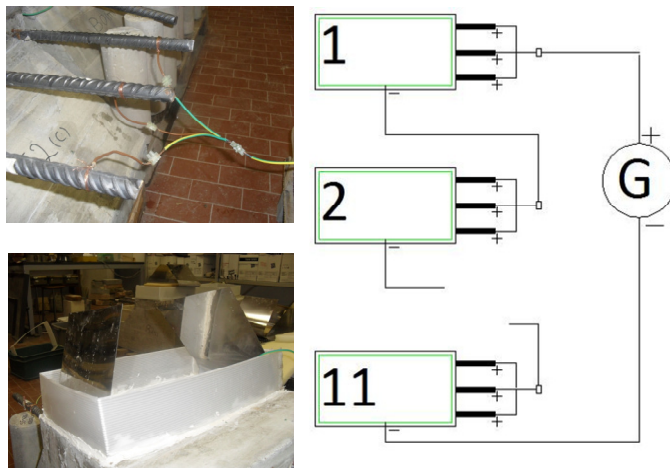


Figure 2. Accelerated corrosion setup.

Three different corrosion levels were investigated, related to the crack propagation:

- Level 1 corresponded to cracks propagating along the main reinforcement; the corrosion level is around 1-2%;
- Level 2 corresponded to the reaching of approximately 10% corrosion;
- Level 3 aiming to reach the delamination of the covers (tests still on their way).

The specimens are of three different types, in relation to the reinforcement arrangement and corrosion:

- type A: main bars corroding while the stirrups are protected by insulating tape;
- type B: specimens without stirrups, only main bar corrosion;
- type C: main bars and stirrups corroding.

## Results

Corrosion attack values were determined theoretically using Faraday's law and *a posteriori* by weight loss measurement. The difference between the two on average were approximately 10%.

Crack widths on the bottom (in the corrosion setup the top) and side cover were measured during the corrosion process using a microscope with a resolution of 0.04mm up to corrosion Level 1. Cracks that were not accessible by the former method, were measured by post-processing digital photographic images of the specimens before the load testing.

### Corrosion Level 1

Between corrosion initiation and level 1 all specimens showed longitudinal cracks along the main bars. The first corrosion cracks opened around 30-50 microns attack. The cover around each bar is cracked radially; either the side or bottom or both covers were cracked. The first cracks to open were on the bottom cover (top cover during corrosion); for these measurements at intervals were made (Fig.3).

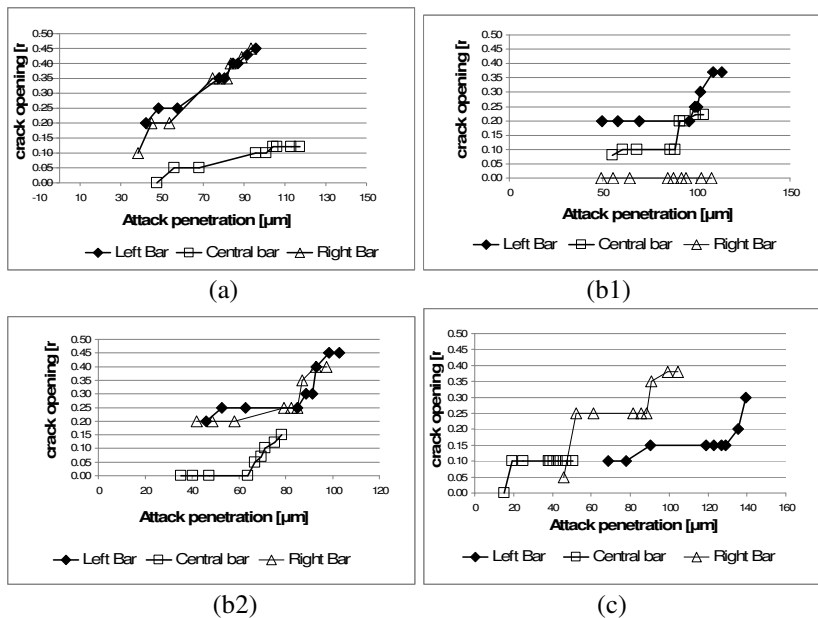


Figure 3. Bottom cover crack opening measurements: (a) with stirrups (not corroding) (b1-b2) without stirrups; (c) with stirrups (corroding).

### Corrosion Level 2

Moving from Level 1 to Level 2, in some specimens part of the radial cracks joined to form a delamination surface connecting two or three bars (Fig.3). The measurements of the bottom cover cracks were suspended because the accumulation of corrosion products made these observations not accurate.

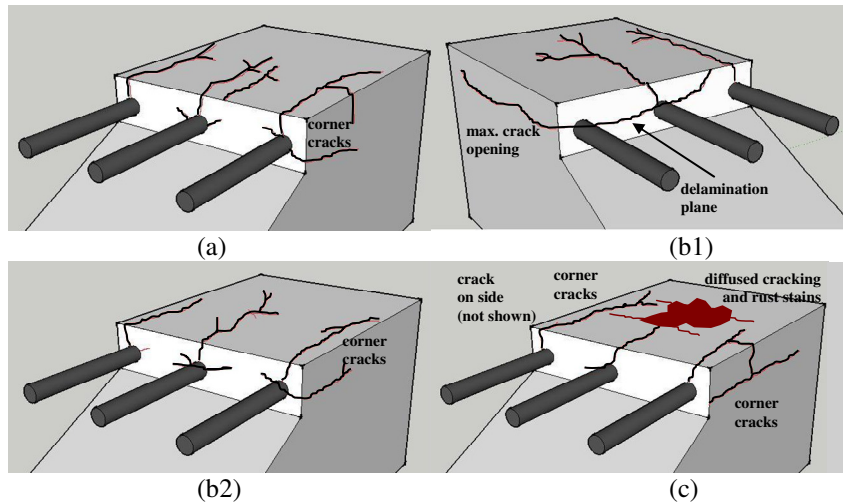


Figure 4. Crack patterns, Level 2: (a) with stirrups (not corroding); (b1-2) without stirrups; (c) with stirrups (corroding; diffused cracks on the top of the specimen not sketched, for clarity of the drawing).

#### Specimens with non corroded stirrups (Type A)

Longitudinal cracks showed in bottom and side covers (Fig.4a). The crack pattern on the front cover is:

- cracks radiating from the bar to the closest point of the outer surface;
- cracks lying in a horizontal plane;
- cracks in inclined planes forming a “V-shaped” pattern.

On the side covers, longitudinal and transverse cracks form.

#### Specimens without stirrups (Type B)

The cracks run mainly along the longitudinal reinforcement (Fig.4b). These specimens showed fewer and wider cracks than those with stirrups. In one of the specimens a delamination plane formed connecting two bars, with a maximum crack width of 1.4mm (Fig.4-b1).

#### Specimens with corroded stirrups (Type C)

Specimens C showed two different crack patterns (Fig4c):



- bottom cover cracking, with corrosion products showing in big stains on the outer surface; many small cracks open, both longitudinally and in other directions (not shown in the drawings);
- initiation of delamination cracks, forming a plane across the bars, and front and side cover cracking.

On the whole the presence of stirrups causes a more complex crack pattern than for specimens without stirrups, both when these are non corroding or corroding. The corrosion level for the C specimens is nominal, because the amount of current involved in the main bars corrosion and that for the stirrups are still unknown, until gravimetric measurements are made on the bars after the tests.

### **Corrosion Level 3**

The ongoing corrosion process is moving towards this level, around 20% corrosion. The formation of delamination planes is initiated in most specimens. The opening of the longitudinal cracks on the bottom cover slows down. The pressure of the corrosion products is acting on a much wider plane, rather than inside the bar hole as it was initially.

## Numerical Modelling

The beam-end specimens were modelled in detailed 3D finite element (FE) analysis. Due to symmetry, half of the specimen was model with 10 mm element size in the finite element program DIANA. Four-node, three-side isoparametric solid pyramid elements were used for concrete, transverse and longitudinal reinforcement. A constitutive model based on non-linear fracture mechanics using a smeared rotating crack model based on total strain is applied for concrete; see [1]. The crack band width was assumed to be equal to the element size; this was later verified in the analyses. For the concrete in tension and compression the models by [2] and [3] were adopted, respectively. The reinforcing steel was modelled based on an isotropic plastic model with Von Mises criterion. The material properties used in the analyses are given in Table I.

*Table I. Material properties used in the analyses.*

Mix	Concrete				Reinforcement		
	$f_{cc}^*$ [MPa]	$f_{ct}$ [MPa]	$G_F$ [N/m]	$E_c$ [GPa]	$f_y$ [MPa]	$E_s$ [GPa]	$f_u$ [MPa]
Reference specimens	29.7	2.33	64.3	29.42	510	200	610
Corroded specimens	27.7	2.19	61.2	28.74	510	200	610

\* The values given are cylinder strength calculated from cubic strength.

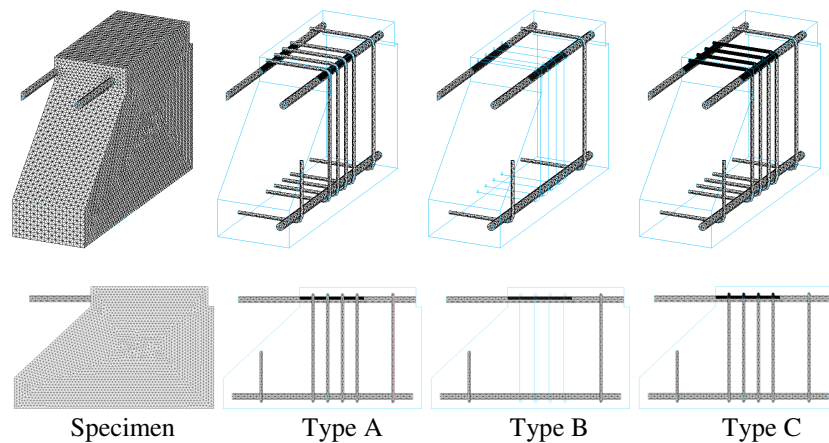


Figure 5. FE model of the beam-end specimen; the shaded bars were subjected to corrosion.

The bond and corrosion models used in the analyses have been earlier developed by Lundgren [4,5]. The modelling method specially suits for detailed 3D FE analyses, where both concrete and reinforcement are modelled with solid elements. The bond model is a frictional model, using elasto-plastic theory to describe the relations between the stresses and the deformations. The corrosion model takes into account the effect of corrosion as the expansion of the corrosion product. The bond and corrosion models were implemented into interface elements which were used to model the interaction between the concrete and reinforcement.

The ratios of volumetric expansion of different typical oxides with respect to the virgin material, given in the literature [6], varies between 1.7 for FeO and 6.15 for  $\text{Fe}(\text{OH})_3 \cdot 3\text{H}_2\text{O}$ . While the value of 2.0, suggested by Molina *et al.* [7], is frequently used in numerical analysis of corroded concrete [8,9,10,11], Bhargava *et al.* [12] proposed a value of 3.39357 based on the available published experimental data. The composition of the rust produced in the tests presented here is not identified yet. Since the corrosion model used in these analyses has been calibrated with a value of 2 for volumetric expansion of rust; therefore, the same value was chosen for all analyses presented here.

Similar to the experiments, the longitudinal bars were subjected to corrosion attack from bottom cover, i.e. half of the cross-section is affected by corrosion; see Fig.5. The top leg of the stirrups was subjected to corrosion all around the cross-section. The vertical leg of the stirrups was corroded up to the half of the longitudinal bar section. Unlike the experiment, the same corrosion penetration was imposed on all bars; this level of corrosion corresponds to the corrosion penetration of the tested bar in the pull-out test.

An incremental static analysis was performed using a Newton-Raphson iterative scheme to solve the non-linear equilibrium equations. In a phased analysis, first the corrosion attack was applied. Then the external load was gradually applied on the tested bar as prescribed displacement. The outcome of the latter phase is presented in the companion paper subtitled “Paper 2. Anchorage Capacity”.

### Results

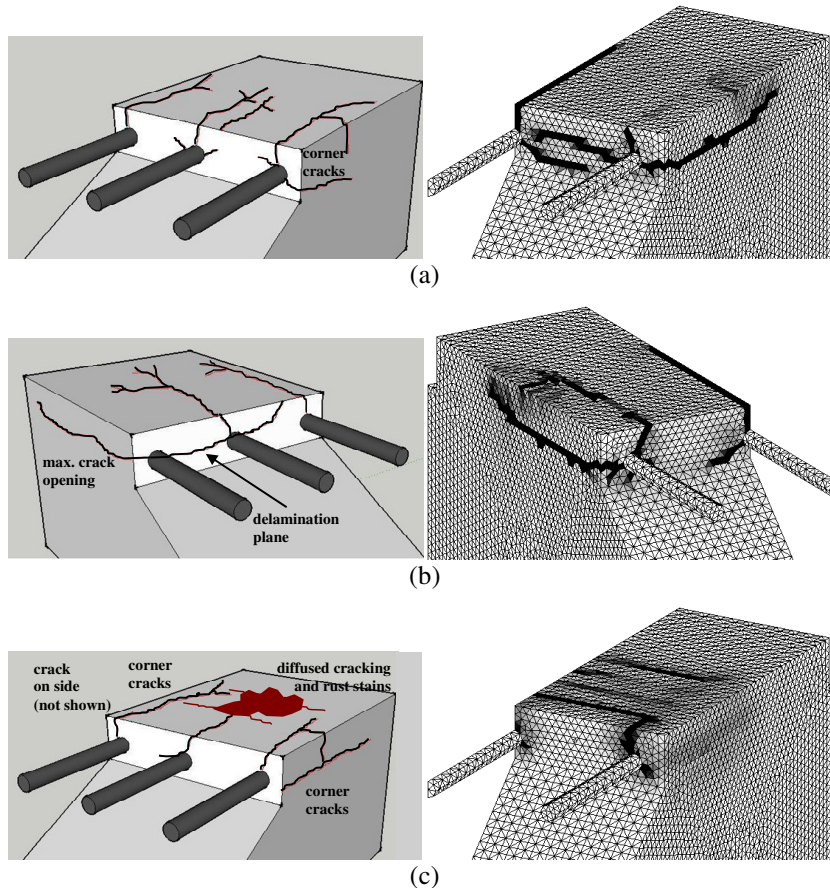


Figure 6. Comparison of experimental and numerical (half of the specimen) crack patterns: (a) Type A; (b) Type B; (c) Type C.

The longitudinal cracking and the delamination planes forming are simulated in Fig.6a,b with and without stirrups. The corrosion of stirrups (Fig.6c) fractures the

cover transversely, with a damage pattern frequently observed in real structures. In the tests this part of the cover is densely cracked (not shown in left figure).

Three main cover spalling patterns can be observed in the numerical analysis:

- The corrosion-induced cracks, initiated from corner and middle bars, propagate across the cross-section and form a delamination plane. This type of pattern is dominant in the specimens of Type A (non-corroding stirrups).
- In the absence of stirrups, the corrosion-induced cracks around the corner bars propagate in a direction with the least resistance. Therefore, a corner cover spalling takes place; this is clearly seen in the specimens of Type B (without stirrups).
- A different pattern is observed when both longitudinal and transverse bars are corroding, specimens of Type C. This rises to a situation in which wide cracks appear transversely due to corroding stirrups before any of the former spalling patterns occurs. Here a more local cover spalling pattern, mainly spalling of the concrete between stirrups, shapes. As the concrete cover is smaller over the stirrups, the splitting cracks appear for relatively low corrosion penetration.

Generally, the crack patterns achieved in the numerical analyses agree well with the observation from experiments. In the present paper, quantitative comparison of the cracks, i.e. crack width, is not intended. But it is important to note that the amount of corrosion penetration needed to cause cover spalling was rather low in the numerical analyses compared with what was observed in the experiments. This is believed to be due to rust flowing into the cracks and slowing down the rate of the splitting pressure built up around the corroding bar. This phenomenon has a more significant effect for larger corrosion attacks when wide cracks allow for more rust to escape. The present version of the corrosion model does not include the flow of rust into the cracks but this will be one of the main concerns in further development of the model.

## Conclusions

An experimental program on bond of corroded bars in reinforced concrete has been started, investigating high corrosion levels, cover cracking and delamination and the corrosion of the stirrups. The results of the artificial corrosion process have been presented in this first of two parts of the paper.

A numerical 3D finite element model has been setup to simulate the tests. The results correspond to the experimental observations, opening the way to the modelling of the pull-out bond tests performed on the same specimens (Part 2 of this paper).

The aim is to assess both experimentally and numerically the bond of the reinforcement in heavily corroded concrete specimens. In particular the study aims at understanding whether neglecting the effect of corroded stirrups on crack

initiation, crack propagation and cover delamination may lead to overestimation of the load-carrying capacity of the corroded structure.

## References

- [1] Diana, DIANA Finite Element Analysis, User's Manual, release 9.1, in: (Eds.), TNO Building and Construction Research, Delft, Netherlands, 2006, pp.
- [2] D. A. Hordijk, Local Approach to Fatigue of Concrete, Doctoral thesis, Delft University of Technology, Delft, Netherlands, 1991.
- [3] E. Thorenfeldt, A. Tomaszewicz, J. J. Jensen, Mechanical properties of high-strength concrete and applications in design, Conference on Utilization of High-Strength Concrete, Stavanger, Norway, 1987,
- [4] K. Lundgren, Bond between ribbed bars and concrete. Part 1: Modified model, Magazine of Concrete Research, 57 (7) (2005) 371-382.
- [5] K. Lundgren, Bond between ribbed bars and concrete. Part 2: The effect of corrosion, Magazine of Concrete Research, 57 (7) (2005) 383-395.
- [6] Y. Liu, R. E. Weyers, Modeling the time-to-corrosion cracking in chloride contaminated reinforced concrete structures, Aci Materials Journal, 95 (6) (1998) 675-681.
- [7] F. J. Molina, C. Alonso, C. Andrade, Cover Cracking as a Function of Rebar Corrosion. 2. Numerical- Model, Materials and Structures, 26 (163) (1993) 532-548.
- [8] D. Coronelli, P. Gambarova, Structural assessment of corroded reinforced concrete beams: Modeling guidelines, Journal of Structural Engineering, 130 (8) (2004) 1214.
- [9] K. Lundgren, Modelling the splitting effects of corrosion in reinforced concrete, Computational Modelling of Concrete Structures, Euro-C Conference, St. Johann, Austria, 2003, Balkema, 491-500.
- [10] K. Zandi Hanjari, Load-Carrying Capacity of Damaged Concrete Structures, Lic. Thesis, Department of Civil and Environmental Engineering, Chalmers University of Technology, Gothenburg, 2008.
- [11] K. Lundgren, A. S. S. Roman, H. Schlune, K. Z. Hanjari, P. Kettil, Effects on bond of reinforcement corrosion, International RILEM workshop on Integral Service Life Modeling of Concrete Structures, 5-6 November 2007, Guimaraes, Portugal, 2007, RILEM Publications S.A.R.L, 231-238.
- [12] K. Bhargava, A. K. Ghosh, Y. Mori, S. Ramanujam, Model for cover cracking due to rebar corrosion in RC structures, Engineering Structures, 28 (8) (2006) 1093-1109.